

## **Development of a Soil Site Ground Motion Database for Australian Seismic Structural Design**

**Yiwei Hu<sup>1,6</sup>, Elisa Lumantarna<sup>2,6</sup>, Nelson Lam<sup>3,6</sup>, Scott Menegon<sup>4,6</sup>, John Wilson<sup>5,6</sup>**

1. Corresponding Author. PhD candidate, Department of Infrastructure Engineering, The University of Melbourne, Parkville, VIC 3010, Australia.  
Email: huyh1@student.unimelb.edu.au
2. Lecturer, Department of Infrastructure Engineering, The University of Melbourne, Parkville, VIC 3010, Australia. Email: elu@unimelb.edu.au
3. Professor, Department of Infrastructure Engineering, The University of Melbourne, Parkville, VIC 3010, Australia. Email: ntkl@unimelb.edu.au
4. Research Fellow, Centre for Sustainable Infrastructure, Swinburne University of Technology, Melbourne, Australia. Email: smenegon@swin.edu.au
5. Professor, Swinburne University of Technology, Sarawak Campus, Kuching, Sarawak, Malaysia. Email: jwilson@swin.edu.au
6. Bushfire and Natural Hazard Cooperative Research Centre, Melbourne, Australia

### **Abstract**

This paper presents the development of a ground motion acceleration database that is specifically established for seismic structural design purpose in Australia. The database particularly focuses on providing abundant accelerograms representing earthquakes with a 500-year and 2500-year return period based on the Australian code spectrum model. Typical soil profiles were derived from borehole records in Melbourne, Sydney and Brisbane to account for the sediment amplification effect on soil sites, considering the site natural period as the main classification parameter. Using the equivalent linear analysis, a suite of MATLAB programs referred to as SUA was validated by comparison with results from SHAKE91 and is applicable for quantity production. The development of this database aims at producing ground motion acceleration time histories that fit in code response spectrums and can be applied in Australia structural design, and is an early attempt for future work with ground motion attenuation models.

**Keywords:** Australian earthquakes, SUA, equivalent linear analysis

## 1. INTRODUCTION

The seismological models are developed to predict ground motion properties in the frequency domain from earthquake magnitude generated at the source of the seismic waves, and to generate a realistic response spectra model. For seismically active regions, the strong instrumented data with various combinations of earthquake magnitude, distance from recording site to the source and site geological condition are sufficient to carry out regression analysis and derive empirical attenuation models. On the other hand, regions of low and moderate seismicity, due to lack of local strong earthquake data, are inclined to use small tremors and aftershocks. The relatively weak ground motion records would induce lower response spectra in the long-period range (displacement), which often controls the seismic design of tall buildings. Therefore, empirical models derived based on purely regression analysis in these regions cannot represent the properties of rare and disastrous strong seismic events. An alternative approach to generate response spectra in regions of lower seismicity is to adopt the well-established seismological models from other regions that share similar tectonic conditions but have abundant data of strong earthquakes. However, research that has been carried out that south-eastern Australia, which is categorised as stable intraplate region and has similar attenuation pattern with the unstable north-western America (Wilkie and Gibson, 1995), results in the conclusion that regional analogy solely considering tectonic condition is unsatisfactory.

Following Brune's work in 1970, Lam and his coworkers incorporated the component attenuation model (CAM) into a response spectrum model to investigate the seismic hazard on rock sites (2000a). CAM accounts for the effect from source and crustal path components and expresses the Fourier amplitude spectrum as a product of several seismological parameters. CAM has the advantage of being able to model each component that would contribute to the attenuation of the seismic shear waves, therefore the lack of strong ground motion records or poor resolutions of instrumented data in low-frequency motions would not influence the accuracy of such model. In this regard, the superiority of CAM compared with conventional empirical models makes it particularly efficient in regions short of indigenous strong records, like most parts in Australia.

In the current Australian Standard 1170.4-2007 for earthquake action, buildings with high importance level, significant sediment effect and structural height, are to be evaluated under Earthquake Design Category (EDC) III using dynamic analysis. For a specific site, appropriate strong ground motion accelerograms recorded on rock sites are selected to have an average response spectrum that approximates the bedrock design spectrum, and are transferred to surface ground motions considering the sediment amplification effect. The resultant surface ground motion time histories are then applied to the structure to capture its behavior at each time step. Most regions and cities in Australia lack well-recorded large earthquake accelerograms to represent destructive seismic event with a return period (RP) of 500 years or 2500 years, causing increasing difficulty to perform dynamic analysis. In some occasions, dynamic analysis would be carried out with casual choice of accelerograms from other countries' earthquake database, some of which may not conform to Australian seismic content. In this study, more reliable accelerograms were collated for direct engineering application based on Australian code response spectra. Currently, the accelerograms have been collated based on the response spectra in accordance with AS1170.4-2007, hence the difference caused by faults and geological conditions was accounted for by using an appropriate earthquake hazard factor depicted in Australia earthquake hazard map.

Future work will include taking into account ground motion attenuation models in the collation of accelerograms to provide more sophisticated ground motion database.

## 2. METHODOLOGY

The overall methodology adopted in this study is to firstly select ground motion accelerograms on rock sites with preferred magnitude-distance (M-R) combinations from the Pacific Earthquake Engineering Research (PEER) Center considering the return period to be 500 or 2500 years (PEER, 2014). Then the accelerograms were scaled to approximate the Australian code response spectrum for generic class B rock. The scaled bedrock accelerograms were used to simulate soil site surface time histories using a MATLAB-based program referred to as SUA (Robinson, Dhu and Schneider, 2006) that employs equivalent linear one-dimensional response analysis to compute regolith site response. The soil profiles, with large diversity in terms of natural period and shear wave velocity, were derived from geotechnical borehole logs in Melbourne, Sydney and Brisbane. The detailed numerical process and soil site accelerogram conduction are presented in this section.

### 2.1 Selection of Ground Motion Accelerogram

As a region of low to moderate seismicity, Australia lacks well-recorded indigenous strong seismic events and ground motion data. Therefore, to construct a database with accelerograms that are representative of Australian seismic source and crustal characteristics, real ground motion records from other countries or regions were selected carefully based on fault type, site geological condition and the magnitude and epicentral distance (M-R) combination. The records were obtained from PEER Center based on the following searching criteria. The preferred fault type is the Reverse/Oblique fault type which is the most common fault type in Australia.  $V_{30}$  was selected to eliminate records from generic soil site conditions.

- Reverse/Oblique fault type;
- Magnitude ranges from 4 to 7;
- Joyner-Boore distance  $R_{jb}$  (defined as the distance to the fault projection to the surface) ranges from 10 to 150 km;
- $V_{30}$  ranges from 600 to 1800 m/s.

A further selection criterion is the M-R combination which would determine the intensity of seismic events. In regions of lower seismicity, explicitly defining the geometry and degree of activity of seismic source zones that would influence the subject site is difficult. In this study, the uniform seismicity approach was adopted that assumes a uniformly distributed circular source zone around the given site (Lam *et al.*, 2000b). Based on the Gutenberg-Richter magnitude recurrence relationship, Eq. (1) is introduced to determine the M-R relationship.

$$M = 5 + \{\log_{10}(2\pi R^2 T_{RP}) - 7 + a_5\}/b \quad (1)$$

The seismicity parameters  $a_5 = 1.6$  and  $b = 0.9$  were assigned to describe a typical moderately active intraplate seismic region (Lam *et al.*, 2000b). Solving Eq. (1) with a set of earthquake magnitude and  $T_{RP}$  equals to 500 and 2500 gives the corresponding range of source-to-site distance. To allow for relative deviation, the distance range for record selection was broadened. For example, for a 500-year-return-period record selection, if the magnitude of the event is

between 5 and 6, the distance criterion allows the  $R_{jb}$  to range between 10 km to 70 km, corresponding to the solution of  $M$  equals to 4 and 7. It is noteworthy that directivity was not considered in this study. Table 1 summarised the appropriate  $R_{jb}$  range for each magnitude range and return period.

**Table 1 500 and 2500 Years Return Period M- $R_{jb}$  Range**

Magnitude Range		500-year-RP $R_{jb}$ Range (km)		2500-year-RP $R_{jb}$ Range (km)	
Min	Max	Min	Max	Min	Max
4	5	10	30	10	15
5	6	10	70	10	30
6	7	30	150	15	90

## 2.2 Scaling Process

The magnitude scaling refers to multiplying the entire acceleration time history by a certain factor to adjust the amplitude of the accelerogram. In this study, magnitude scaling has been applied and the scaling factor was determined based on the response spectral acceleration in accordance with AS1170.4-2007 with a design hazard factor of 0.08 for Melbourne. Taking 500-year-return-period code rock spectrum as an example, the area  $A_s$  under the standard acceleration response spectrum, period ranging from 0.3 second to 1 second, was calculated as the scaling measurement. The reference period lower and upper boundary were chosen considering the majority structural natural period range as illustrated in Figure 1.

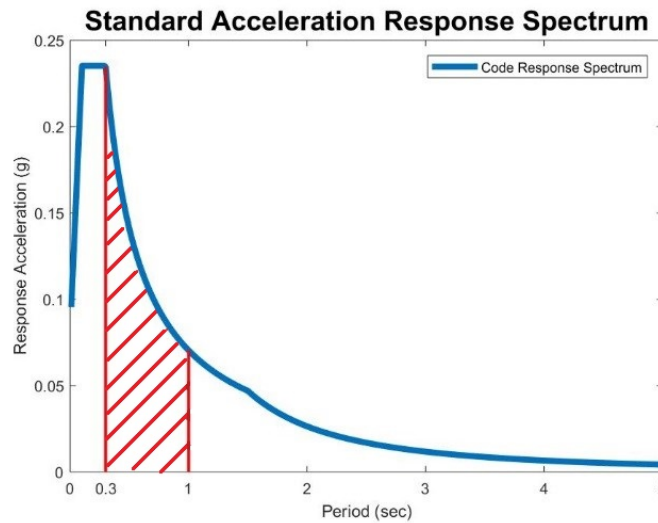


**Figure 1 Demonstration of Standard Scaling Measurement**

For each accelerogram selected in Section 2.1, the area under the response spectrum in the same period range was obtained as  $A_i$ . The ratio of  $A_s$  over  $A_i$  was used as the scaling factor to modify individual accelerogram to approximate the code response spectrum. To avoid losing much of the frequency content of a certain seismic event, the scaling factor was limited to 0.75 to 1.5. Records with a scaling factor outside this range were eliminated from this study. As a result, 16 records were selected with 500 years return period and 15 with 2500 years return period. The response

spectrum of each scaled record is superimposed to the mean response spectrum in Figure 2 (the dynamic properties include response spectral acceleration, RSA; response spectral velocity, RSV and response spectral displacement, RSD). Some humps can be observed from individual response spectrum; however, they are eliminated during the averaging process.

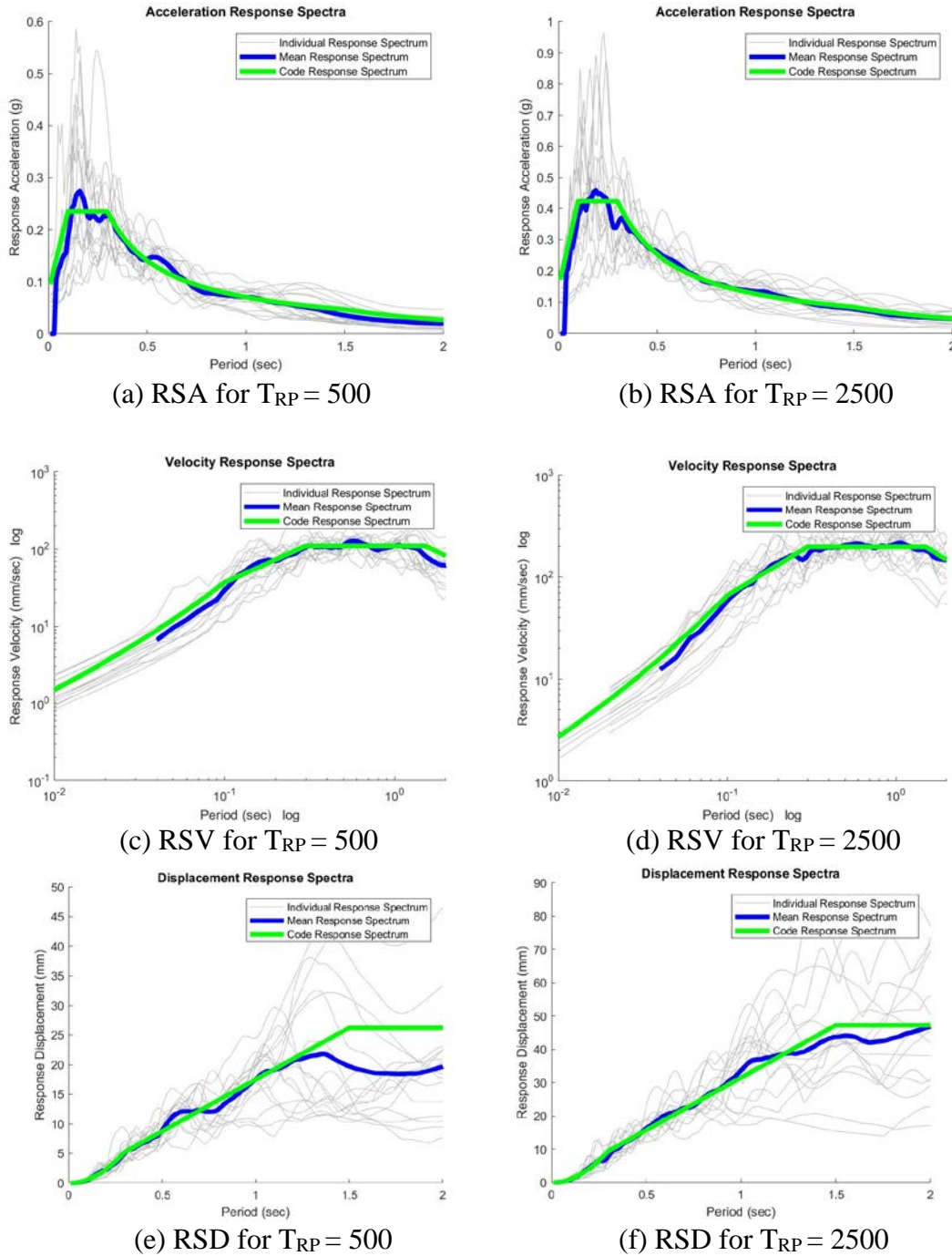


**Figure 2 Individual and Mean Response Spectra for Rock Site Accelerograms**

### 2.3 Soil Profile Generation

This section describes how soil profiles are generated to simulate the soil amplification effect. Compared with the modulus reduction factor, damping ratio or soil density, the sediment amplification factor is more sensitive to the shear wave velocity and thickness of each soil layer (O'Connor *et al.*, 2003). Therefore, extra care must be taken in calculating the shear wave velocity. Firstly, the density of each layer was assigned considering soil type, depth and water content (dry clay density is typically in the range of 1.43 to 2.14 g/cm<sup>3</sup>, wet clay 1.63 to 2.25 g/cm<sup>3</sup>, dry sand 1.32 to 1.63 g/cm<sup>3</sup>, wet sand 1.84 to 2.04 g/cm<sup>3</sup>, dry gravel 1.53 to 1.73 g/cm<sup>3</sup> and wet gravel 2.04 to 2.25 g/cm<sup>3</sup>). Given the ground water level and soil unit weight (based on the density), the vertical effective pressure in the middle thickness for each soil layer can be calculated accordingly. Based on the logging report description on the consistency for both cohesive and non-cohesive soils (and sometimes directly provided in the report by sampling and experiment), the normalised Standard Penetration Test (SPT)  $N_{60}$  value was assumed according to the Queensland Geotechnical Borehole Logging Guideline (2016). Eq. (2)-(4) from PEER Guideline were adopted to estimate shear wave velocity profiles based on the SPT  $N_{60}$  value and vertical effective pressure (Wair, DeJong and Shantz, 2012), where Eq. (2)-(3) were obtained from PEER's study and Eq. (4) from Rollin's research in 1998.

$$V_s = 26 \times N_{60}^{0.17} \times \sigma'_v{}^{0.32} \quad \text{for clay} \quad (2)$$

$$V_s = 30 \times N_{60}^{0.23} \times \sigma'_v{}^{0.23} \quad \text{for sand} \quad (3)$$

$$V_s = 53 \times N_{60}^{0.19} \times \sigma'_v{}^{0.18} \quad \text{for gravel} \quad (4)$$

The bedrock shear wave velocity was adopted based on the average of typical velocity ranges from previous literatures for various rock types for simplification (Koerperich, 1980; Ahmed, 1989; Fasani *et al.*, 2013). To represent a variety of site sediment and rock conditions, 53 borehole records from capital cities across Australia were examined to include various soil depth, site natural period and weighted shear wave velocity. As a result, 53 soil profiles were generated in this study, 5 of which were classified as Class D soils, 4 as Class E soils and the rest as Class C soils, according to the site classification criteria in AS1170.4-2007. The shear wave velocity profiles for the 53 boreholes are presented in Figure 3. The site natural period was defined as the shear-wave travel time through four times the soil thickness (as shown in Eq. (5)), and the shortest and longest natural period obtained in this study is 0.06 and 0.81 second, respectively.

$$T_n = 4 \times H / V_s \quad (5)$$

where H is the total depth of the site soil and  $V_s$  is the weighted average shear wave velocity.

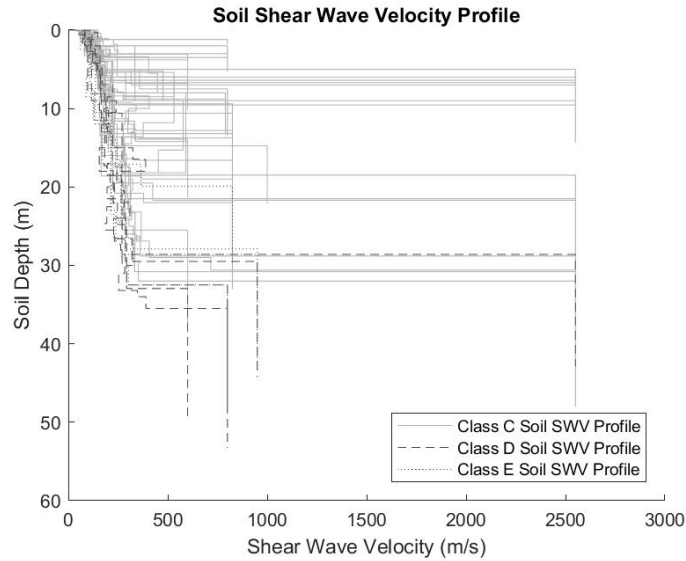


**Figure 3 Soil Shear Wave Velocity Profile**

## 2.4 Soil Amplification

The presence of soils and extremely weathered rocks can amplify the intensity of ground motions significantly due to decrease in shear wave velocity compared with bedrock, thus soil amplification effect is a vital component in seismic structural design and analysis. This effect was modelled in this study using the equivalent linear approach to describe the vertical propagating shear wave in a one-dimensional manner. There are many widely-accepted programs using this technique to transfer the bedrock ground shaking in to soil surface acceleration time history, for example SHAKE91 (Idriss and Sun, 1992), EERA (Bardet, Ichii and Lin, 2000) and SUA (Robinson, Dhu and Schneider, 2006). The MATLAB-based SUA program employed in this study has its advantage in transparency and allow for quantity production with loop routines compared with SHAKE and EERA.

To account for the soil non-linear response under severe strain, the modulus reduction and damping ratio curves were defined by the soil plasticity indices PI according to Hardin and Drnevich Model (1972). It is noteworthy that the ratio between the effective strain and maximum strain was determined relevant to the earthquake magnitude using Idriss and Sun's estimation equation (1992), as shown in Eq. (6), rather the default value of 0.65. The iterative convergence rate was selected to be 5% in a maximum of 50 trials.

$$\gamma_{eff}/\gamma_{max} = (M - 1)/10 \quad (6)$$

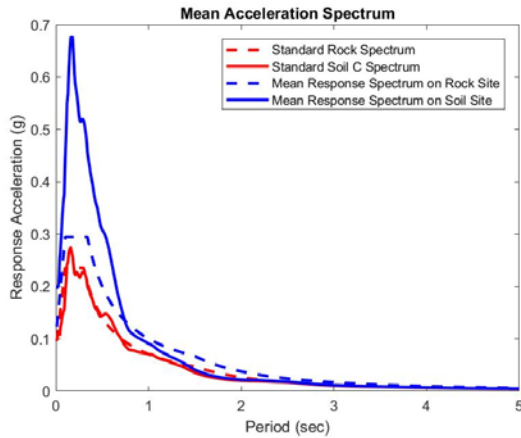
## 3. RESULT AND DISCUSSION

### 3.1 Mean Response Spectra for Three Soil Classification

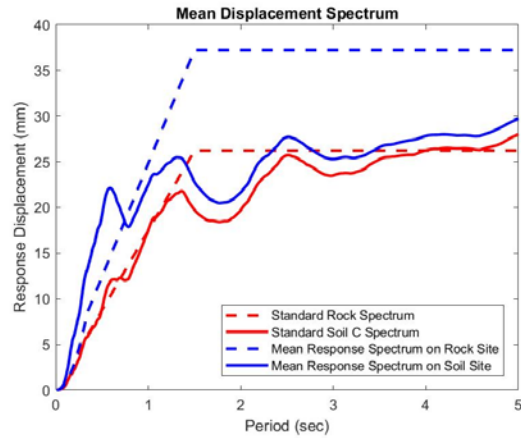
The response spectra on soil sites were averaged based on their site classification to observe the general amplification effect of sediments and to compare the mean response spectra with code

response spectra. The period range examined here was extended to 5 seconds to obtain low-frequency response and to include possible long-period response spectral displacement reduction. During the averaging process of the response spectra in difference sites, the true response behavior is lost (Lam and Wilson, 2004). However some resonance effect can still be observed in short-period range ( $RSA_{max}$ ) for Site Class C and in long-period range ( $RSD_{max}$ ) for Site Class E.

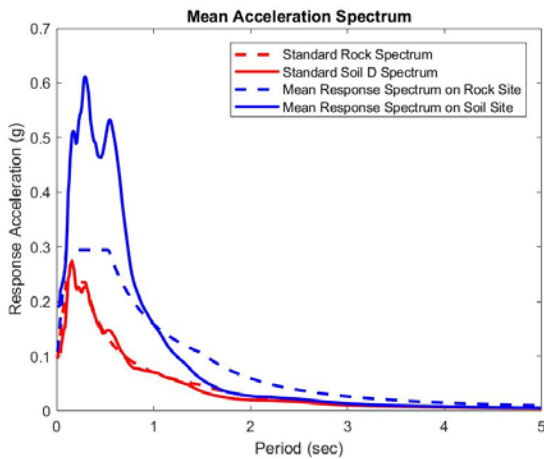
To construct the response spectra, two corner periods have been defined based on an extensive study on attenuation model in Australia (Lam *et al.*, 2000b). The determined corner periods are designed for rock site situation but are extended to soil sites in AS1170.4-2007. From observation of Figure 4 (c) and (d), the first and second corner periods, which respectively define the periods at which the maximum acceleration and displacement occur, could be different from the rock site corner periods. However, revising the standard response spectra is outside the scope of this study, and the mean response spectra are presented here for demonstration purpose only. The red lines in Figure 4 represent the code spectra for rock site and three classes of soil sites from AS1170.4-2007.



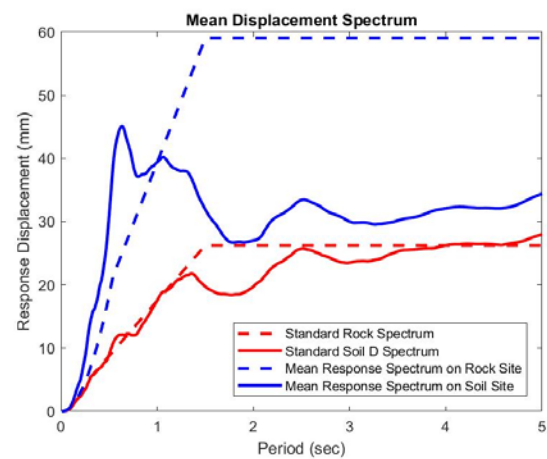
(a) Mean RSA for Class C Sites



(b) Mean RSD for Class C Sites



(c) Mean RSA for Class D Sites



(d) Mean RSD for Class D Sites



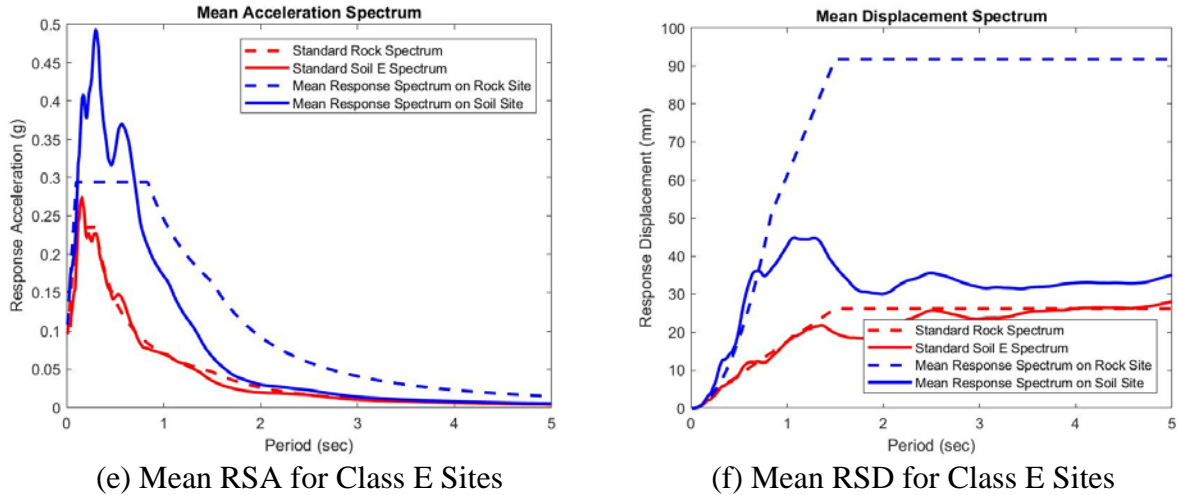


**Figure 4 Mean Response Spectra with 500-year Return Period**

### 3.2 Comparison of Soil Amplification Effect

Unlike other international code of practice (IBC, 2006) that utilises the average shear wave velocity in the surface 30 meters depth as the site classification criteria, the Australian Standard distinguishes site sub-soil class based on the combination of soil depth to the bedrock as well as the average shear wave velocity in the whole profile. The definitional difference between Class C shallow soil site and Class D deep or soft soil site in AS 1170.4 is whether the low-amplitude natural period exceeds 0.6 seconds. The influence of site natural period on the soil amplification effect was investigated in this study. As mentioned in section 2, the natural site periods calculated from soil profiles range between 0.06 to 0.81 second. 4 soil profiles with gradually increasing low-amplitude period have been selected and the corresponding response spectra are compared herein. The natural site periods  $T_n$  in second and the associated site classes are 0.099 (Class C), 0.294 (Class C), 0.504 (Class C) and 0.683 (Class E). The shear wave velocity profile for the four sites is presented in Figure 5. As the average shear wave velocity does not vary much amongst the soil profiles (ranges from 142 to 170 m/s), the significant difference addressed here was contributed by the soil depth and rock velocity.

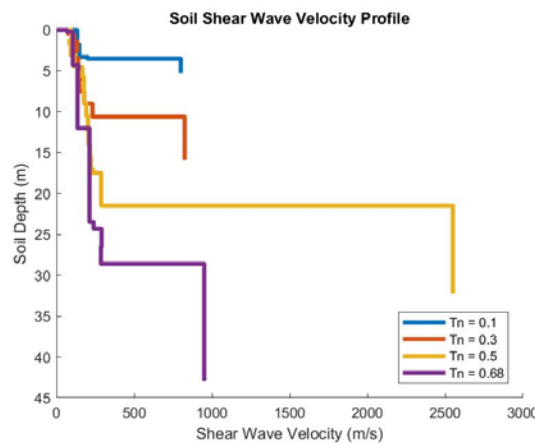


**Figure 5 Shear Wave Velocity Profile of Four Site with Increasing Natural Period**

As shown in Figure 6, site 3 with a natural site period of 0.5 second has the greatest amplification effect in the low-period range. The reason behind this is that site 3 has the highest rock shear wave velocity compared with the other three sites (by 3 times). When the earthquake shear waves reflected from the soil-air interface reach the bedrock-soil interface, part of the energy would be reflected back to the soil layer and the rest would transmit through the interface and travel down into the earth. The energy loss at the bedrock-soil interface is defined as radiation damping and is related to the impedance ratio, which strongly depends on the rigidity of the bedrock. Namely, the more rigid the rock, the less energy would be lost in radiation damping, and thus stronger the ground motion intensity on soil site.

Observation between plot (a) and (b) in Figure 6 gives clear signs of period shift in soils due to large cyclic strain induced by severe ground shaking. The second peak in the graphs represents the resonance effect at site period. Figure 6 shows increasing site period with the increasing earthquake intensity. Previous research has pointed out that the period shift factor is related to the earthquake intensity, shear wave velocity and soil plasticity indices (Tsang, Chandler and Lam, 2006). A preliminary check was performed based on recommended values by Lam and Wilson (1999). In Eq. (5) and (6),  $T_g$  is the fundamental site period in an earthquake and  $T_i$  is the initial low-amplitude site period.  $RSA_{T_i}$  represents the rock response spectral acceleration at the initial site period in  $m/s^2$ . Results are summarised in Table 2 and 3. The equations tend to overestimate the shifted periods, which are more obvious considering smaller earthquakes (RP = 500 years). It is noteworthy that for site 4, which is a mixture of clay and sand, the fundamental site period associated with 500 years return period motions is closer to the estimated shifted site period for cohesive soil (Eq. (7)) whilst the ground motions associated with 2500 year return period show site fundamental period that is closer to the estimated fundamental period of cohesionless soil (Eq. (8)).

$$\frac{T_g}{T_i} = 1.05 + 0.1 \times RSA_{T_i} \quad \text{for cohesive soil} \quad (7)$$

$$\frac{T_g}{T_i} = 1.3 + 0.1 \times RSA_{T_i} \quad \text{for cohesionless soil} \quad (8)$$

**Table 2 Period Shift Factor for 500-Year Return Period**

Site Number	Initial Period (s)	Major Composition	RP = 500 yrs $RSA_{T_i}$ ( $m/s^2$ )	Shifted Period from Eq. (7)(8) (s)	Shifted Period from Spectra (s)	Period Difference (%)
1	0.1	Clay	2.31	0.13	0.11	18.18
2	0.3	Sand	2.30	0.46	0.32	43.75
3	0.5	Clay	1.38	0.59	0.44	34.09
4	0.68	Mixture* <sup>1</sup>	1.02	0.95	0.62	53.23
4	0.68	Mixture* <sup>2</sup>	1.02	0.78	0.62	25.81

**Table 3 Period Shift Factor for 2500-Year Return Period**

Site Number	Initial Period (s)	Major Composition	RP = 2500 yrs RSA <sub>Ti</sub> (m/s <sup>2</sup> )	Shifted Period from Eq. (7)(8) (s)	Shifted Period from Spectra (s)	Period Difference (%)
1	0.1	Clay	4.15	0.15	0.12	25.00
2	0.3	Sand	4.14	0.51	0.5	2.00
3	0.5	Clay	2.49	0.65	0.55	18.18
4	0.68	Mixture* <sup>1</sup>	1.83	1.01	1	1.00
4	0.68	Mixture* <sup>2</sup>	4.15	0.84	1	16.00

\*<sup>1</sup>Site 4 composites both clay and sand, both equations are applied. The row marked with \*<sup>1</sup> shows results from Eq. (7); with \*<sup>2</sup> shows results from Eq. (8).

As presented in Figure 6, although some de-amplification effect can be observed in short-period range with 2500-year return period ground motions, the ground movement was found to be enhanced on soil site in the long-period range. There is a positive correlation between the maximum spectral displacement amplification factor, defined as the maximum ratio between RSD on soil site and RSD on rock site, and the initial low-amplitude site period. As described before, the average shear wave velocity is similar for the four sites, deeper soil (resulting in higher natural site period) allows for the inelastic deformation to increase the amplitude of shear waves.

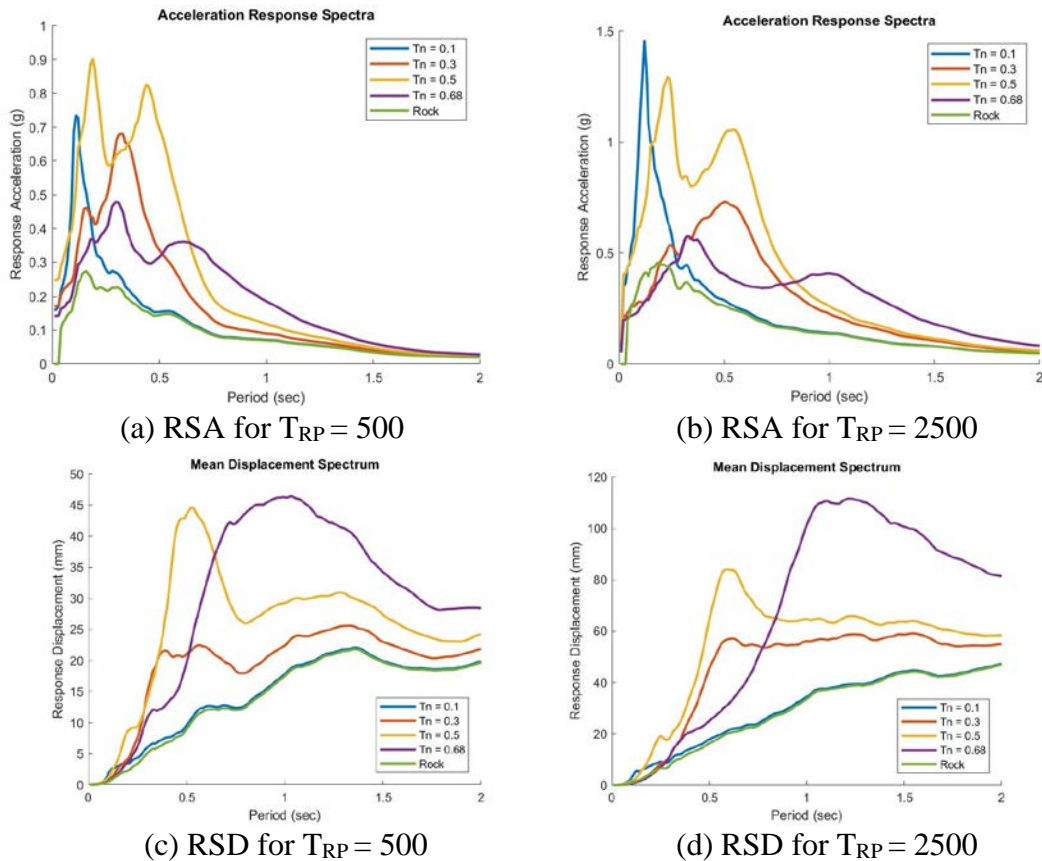


**Figure 6 Mean Response Spectra for Rock Site and Subject Soil Sites**

#### 4. Conclusion

The purpose of this study is to develop a database with accelerograms for dynamic analysis in structural design. To achieve this aim, rock site ground motion time histories were selected to have appropriate M-R combinations and scaled to approximate the rock response spectra according to AS1170.4-2007. Then the accelerograms on rock sites were used to simulate ground motions on soil sites using one-dimensional equivalent linear analysis to account for soil amplification effect. The soil profiles used in the analyses were derived from borehole log records that were obtained from locations in capital cities across Australia. In the limit of length, the accelerograms generated on soil site are not provided in this conference paper but will be available from the University of Melbourne website (the ground motion database is not yet completed).

This study is a preliminary attempt to generate ground motion time histories that are representative of Australian seismic conditions. Crustal and geological condition variability across the continent will be the emphasis of the authors' future work.

#### ACKNOWLEDGEMENT

The support of the Commonwealth Australia through the Cooperative Research Centre program and the Australian Research Council Discovery Project (DP180101593) is gratefully acknowledged.

#### 5. REFERENCE

- Ahmed, H. (1989). Application of mode-converted shear waves to rock-property estimation from vertical seismic profiling data. *Geophysics*, 54(4), 478-485.
- Bardet, J. P., Ichii, K., & Lin, C. H. (2000). User's manual for EERA: A computer program for Equivalent-linear Earthquake Site Response Analysis. *Los Angeles, California, USA: University of Southern California*.
- Brune, J. N. (1970). Tectonic stress and the spectra of seismic shear waves from earthquakes. *Journal of geophysical research*, 75(26), 4997-5009.
- Fasani, G. B., Bozzano, F., Cardarelli, E., & Cercato, M. (2013). Underground cavity investigation within the city of Rome (Italy): a multi-disciplinary approach combining geological and geophysical data. *Engineering geology*, 152(1), 109-121.
- Hardin, B. O., & Drnevich, V. P. (1972). Shear modulus and damping in soils: design equations and curves. *Journal of Soil Mechanics & Foundations Div*, 98(sm7).
- IBC, I. (2006). International building code. *International Code Council, Inc. (formerly BOCA, ICBO and SBCCI)*, 4051, 60478-5795.
- Idriss, I. M., & Sun, J. I. (1992). User's Manual for SHAKE91. *Center for Geotechnical Modeling, Department of Civil Engineering, University of California, Davis*.

Koerperich, E. A. (1980). Shear Wave Velocities Determined from Long-and Short-Spaced Borehole Acoustic Devices. *Society of Petroleum Engineers Journal*, 20(05), 317-326.

Lam, N., & Wilson, J. (1999). Estimation of the site natural period from a borehole record. *Australian Journal of Structural Engineering*, 1(3), 179-200.

Lam, N., Wilson, J., Chandler, A., & Hutchinson, G. (2000a). Response spectral relationships for rock sites derived from the component attenuation model. *Earthquake engineering & structural dynamics*, 29(10), 1457-1489.

Lam, N., Wilson, J., Chandler, A., & Hutchinson, G. (2000b). Response spectrum modelling for rock sites in low and moderate seismicity regions combining velocity, displacement and acceleration predictions. *Earthquake engineering & structural dynamics*, 29(10), 1491-1525.

Lam, N. T. K., & Wilson, J. (2004). Displacement modelling of intraplate earthquakes. *International Seismology and Earthquake Technology Journal (invited paper for the special issue on Performance Based Seismic Design)*.

O'Connor, A., Dhu, T., Jones, A., Robinson, D. (2003) *Analysis of variability in regolith site response models: Investigation into the variability of current site response models for seismic modelling in the Newcastle and Lake Macquarie area*. Canberra: Geoscience Australia

PEER. (2014). Pacific Earthquake Engineering Research (PEER) Ground Motion Database. [http://peer.berkeley.edu/peer\\_ground\\_motion\\_database](http://peer.berkeley.edu/peer_ground_motion_database)

Queensland Department of Transport and Main Roads (2016). Geotechnical Borehole Logging Guideline. <https://creativecommons.org/licenses/by/3.0/au/>

Robinson, D., Dhu, T., & Schneider, J. (2006). SUA: A computer program to compute regolith site-response and estimate uncertainty for probabilistic seismic hazard analyses. *Computers & geosciences*, 32(1), 109-123.

Rollins, K. M., Evans, M. D., Diehl, N. B., & III, W. D. D. (1998). Shear modulus and damping relationships for gravels. *Journal of Geotechnical and Geoenvironmental Engineering*, 124(5), 396-405.

Standard, A. AS 1170.4-2007. *Structural Design Actions, Part, 4*.

Tsang, H. H., Chandler, A. M., & Lam, N. T. (2006). Simple models for estimating period-shift and damping in soil. *Earthquake engineering & structural dynamics*, 35(15), 1925-1947.

Wair, B. R., DeJong, J. T., & Shantz, T. (2012). *Guidelines for estimation of shear wave velocity profiles*. Pacific Earthquake Engineering Research Center.

Wilkie, J., & Gibson, G. (1995). Estimation of seismic quality factor Q for Victoria, Australia. *AGSO Journal of Geology & Geophysics*, 15(4), 511-517.